Journal of Molecular Structure 1250 (2022) 131904

Contents lists available at ScienceDirect

Journal of Molecular Structure

journal homepage: www.elsevier.com/locate/molstr

Hydrogen-bonded supramolecular assemblies of folic acid with simple hexoses

Magdalena Ceborska[a,*], Kajetan Dąbrowa[b], Jakub Cędrowski[c], Magdalena Zimnicka[b]

[a] Institute of Physical Chemistry, Polish Academy of Sciences, Kasprzaka 44/52, 01-224, Warsaw, Poland
[b] Institute of Organic Chemistry, Polish Academy of Sciences, Kasprzaka 44/52, 01-224, Warsaw, Poland
[c] Faculty of Chemistry, University of Warsaw, Pasteura 1, 02-093, Warsaw, Poland

ARTICLE INFO

Article history:
Received 5 July 2021
Revised 19 October 2021
Accepted 7 November 2021
Available online 10 November 2021

Keywords:
Folic acid
Monosaccharides
Hydrogen bonded associates
Supramolecular chemistry

ABSTRACT

Simple D-hexoses such as D-glucose, D-mannose, and D-galactose were found to form supramolecular complexes with folic acid (FA) in phosphate-buffered saline solution (PBS, pH 7.4) and in the gas phase. Pterin subunit of FA was found to be essential for the molecular assembly with hexoses, whereas PABA (p-amino benzoic acid) and GLN (glutamic acid) subunits of FA have virtually no effect on assembly formation. Experimental measurements along with DFT theoretical calculations reveal that hexose-FA assemblies are stabilized by three complementary hydrogen bonds between pterin subunit of FA and 3,4,6-trihydroxyl moiety of hexose.

1. Introduction

Folic acid (FA, vitamin B9, Fig. 1) is an essential compound for various metabolic and biochemical processes in human body. It plays significant role in the synthesis of purines and pyrimidines, as well as in the replication, and methylation of DNA [1]. FA is involved in various drug delivery systems for anticancer therapies [2] due to its uptake by the folate receptor-positive cancer cells. The chemical structure of FA contains *p*-aminobenzoate (PABA) scaffold linked to a pterin ring (PTN) and glutamic acid (GLU) moieties. It is often treated as a model for antifolates [3], compounds structurally related to FA, designed to target and inhibit folate dependent enzymes, inducing inhibition of nucleotide biosynthesis and subsequent cell death [4], used in various anticancer treatments [5].

FA in physiological conditions exists as dicarboxylate anion ($pKaCOOH\_\alpha = 2.35$, $pKaCOOH\_\alpha = 4.56$) [6], and thus folate sensing is mostly performed *via* molecular recognition of carboxylate groups [7].

Generally, carboxylate recognition is mainly achieved by utilization of charged (e.g. metal cations, guanidinium [8], amidinium [9], imidazolium [10], and pyridinium groups [11]) or neutral (e.g. urea [12], thiourea [13], amide [14], and pyrrole [15]) binding groups.

Recombinant human dihydrofolate reductase (DHFR) binds the glutamate part of folate *via* an arginine residue [16], while in the bacterial proteins R67 DHFR [17] and thymidylate synthase (TS) [18] the glutamate part of folate is bound to the ammonium group of lysine. Another solution for binding FA and antifolates is their complexation with supramolecular receptors such as cucurbiturils [19], calixpyridiniums [20], calixresorcinarenes [21], or squaramido-based receptors [22].

Our previous studies proved that native cyclodextrins (CDs) are good receptors for folic acid [23]. α–cyclodextrin (α–CD) and α–cyclodextrin (α–CD) form pseudorotaxane inclusion structures, while α–cyclodextrin (α–CD) forms with FA weekly bound exclusion-type associate, as confirmed by ^{1}H NMR and Ion Mobility Mass Spectrometry (IM-MS).

Usually, efficient binding of carbohydrates in water is very difficult due to the fact that possible interactions with other organic molecules compete with solvation by water molecules being both hydrogen bond donor and acceptors [24]. Even lectins, the predominant class of carbohydrate-binding proteins, bind monosaccharides with K_as of $\sim 10^3$ M^{-1} [25]. Nevertheless, based on the knowledge that FA may interact with the outer shell hydroxyl groups of cyclodextrins (macrocyclic hosts consisting of D-glucose subunits joined by α-1→4 glycosidic bonds) and that dextrins (linear polymers of D-glucose units linked by α-(1→4) or α-(1→6) glycosidic bonds) are able to bind carboxylate anions [26] we decided to investigate if also simple hexoses model such as D-glucose could bind folic acid in water. Additionally, based on previous literature

* Corresponding author.
E-mail address: mceborska@ichf.edu.pl (M. Ceborska).

https://doi.org/10.1016/j.molstruc.2021.131904

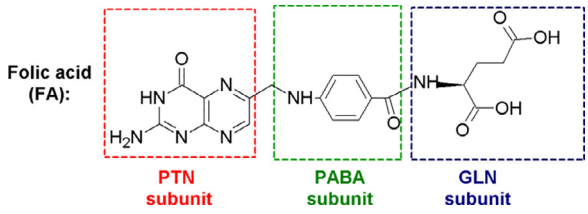

Fig. 1. Chemical structure of folic acid (FA) and its subunits: pterin (PTN), *p*-aminobenzoate (PABA), and glutamic acid (GLN) moieties.

data concerning binding of simple sugars in water, we assumed that binding of FA with hydroxyl groups of studied carbohydrates may also occur *via* interactions with amino groups [27].

In our study we applied the most common hexoses: D-glucose (**G1a**), D-mannose (**G2a**) and D-galactose (**G3a**) which differ in the spatial position of the hydroxyl groups. Application of three stereoisomers should enable the estimation of which hydroxyl groups are responsible for the formation of associates with folic acid. Further studies with their derivatives protected at anomeric positions (methyl α-D-glucoside (**G1b**), methyl α-D-mannoside (**G2b**), and methyl α-D-galactoside (**G3b**) should give an insight into possible role of anomeric hydroxyl group on the binding mode of folic acid.

The complexation studies were performed in solution (phosphate buffered saline, PBS, pH=7.4) and in the gas phase. PBS was used as a solvent of choice due to its wide application in biological systems, as it is isotonic and nontoxic to the majority of cells. In order to examine if the investigated complexes could also be formed in the solid state, we performed Differential Scanning Calorimetry (DSC) and Thermogravimetric (TG) analyses. To prove the identity of the complexes which are formed between simple hexoses and FA, as well as with its subunits, mass spectrometry studies were performed. In addition, the order of stabilization of the investigated complexes in the gas phase was established to gain insight into their intrinsic, solvent-free origin of the stability.

3. Materials and methods

2.1. Reagents

All reagents were of reagent-grade quality. Folic acid, pterin, carbohydrates, and reagents for the synthesis of **H3** were purchased from Sigma-Aldrich and Carbosynth, and were used as received.

2.2. Synthesis of *N-[4-(*methylamino*)*benzoyl*]-L-glutamic acid (H3)*

N-(4-N-methylaminobenzoyl)-L-glutamic acid diethyl ester (200 mg, 0.6 mmol) was dissolved in MeOH-THF-H_2O (15 mL, 1:1:1 v/v/v) solvent mixture. Then LiOH (70 mg, 2.4 mmol, 4 equiv) dissolved in water (2 mL) was added and the reaction was stirred for 48 h at rt. Then glacial acetic acid (1 mL) was added and the reaction was stirred for 30 min. The solvent was evaporated under vacuum yielding white residue which was suspended in EA (~30 mL), filtered through G4 glass filter, and washed with EA (20 mL). The filtrate was dried over sodium sulfate and evaporated under vacuum yielding (140 mg, 83%) of target product H3. ^{1}H NMR (400 MHz, DMSO-d_6) δ 7.82 (*s*, 1H), 7.67 (*d*, J = 8.2 Hz, 2H), 6.50 (*d*, J = 8.3 Hz, 2H), 6.19 (*s*, 1H), 4.21 (*d*, J = 5.3 Hz, 1H), 2.68 (*s*, 3H), 2.05–1.89 (*m*, 2H), 1.96–1.83 (*m*, 2H). ^{13}C NMR (100 MHz, DMSO-d_6) δ 179.9, 177.2, 165.6, 152.1, 128.7, 121.3, 110.4, 54.5, 30.7, 29.4, 24.9–24.8* (* signal is covered by residual solvent). ESI HR-MS calc. for $C_{13}H_{15}N_2O_5$ $[M+H]^+$ 279.0981 found 279.0971.

2.3. UV-Vis measurements

The absorption spectra of **FA, H2**, and **H3** and their respective associates with carbohydrates were recorded using Evolution 220 UV/VIS spectrometer (Thermo Scientific) at 298 K in the range 250–450 nm. All measurements were performed in phosphate-buffered saline (PBS, pH=7.4).

UV-Vis titration experiments

The changes in absorption spectra of **FA, PTN**, and **H3** were measured as a function of varying carbohydrate concentration (0 – 0.01 M). The guest concentration was held constant at $3.8\cdot10^{-5}$ M for **FA**; $6.3\cdot10^{-5}$ M for **PTN**, and $5.1\cdot10^{-5}$ M for **H3**. The association constants (K_a's) were calculated using HypSpec program [28] and different binding equilibria between **FA, PTN**, and **H3** (H) and corresponding carbohydrates (**G**) were considered. The experimental data were tested against all the simplest 1:1 (H:G) binding model and mixed 1:1 + 1:2 (H:G) or 1:1 (H:G) + 2:1 (H:G) binding models to establish a proper stoichiometry and association constants for all studied cases.

2.4. Thermogravimetry (TG) and differential scanning calorimetry (DSC)

TG was performed using a TGA Q50 instrument (TA Instruments) in nitrogen (nitrogen flow was set as 100 ml/min). 3–9 mg samples were heated from 25 to 300 °C in platinum vessel with heating rate 5 °C/min.

DSC measurements were performed using a DSC apparatus Q20 (TA Instruments) in nitrogen (nitrogen flow 100 ml/min). The samples (~3–7.5 mg) were heated from 25 to 300 °C in non-hermetic, covered aluminum pans with heating rate 5 °C/min.

2.5. Molecular modeling

The intrinsic, gas-phase conformations of neutral molecules (**H2** tautomers, hexoses **G1**-**G4**, and **H2**-hexoses associates) were obtained *via* comprehensive molecular mechanics simulations with MMFF force field utilizing the Monte-Carlo algorithm, implemented in the molecular modeling package Spartan'18 [29], followed by the density functional theory calculations using the *Gaussian 16 Rev. B.01* suite of programs. Optimized geometries of local minima and their energies (ΔG at 1 atm and 298.15 K) were obtained using Becke's hybrid functional (B3LYP) [30] supplemented with D3 Grimme's empirical dispersion correction and 6–311++(d,p) basis set. Harmonic frequency analysis was used to confirm the nature of stationary points as local minima (all frequencies real). A quasi-rigid rotor-harmonic oscillator approximation (RRHO) was used to account for low-frequency vibration modes (ν < 100 cm^{-1}) and to obtain the correct entropy values. The protonated structures were obtained as a result of extensive search of the lowest-energy conformations, while varying the positions of the hydrogen atom in the B3LYP-D3 optimized neutral molecules and complexes. Proton affinities were calculated as the negative enthalpy change (298 K) on the gas-phase protonation reaction.

In order to account for the solvent effect on the conformations and energies of the studied supramolecular assemblies a conductor-like polarizable continuum model (C-PCM) using water (ε = 78.30) was employed. Four lowest-energy tautomers of pterin (**H2**) were subjected to comprehensive molecular mechanics simulations, as in the gas-phase calculations, using the Spartan'18 software package [29]. The geometries of obtained **PTN**-monosaccharide assemblies (up to 200 conformers) were then recalculated at higher level of theory (DFT/B3LYP-G3/6-31G(d)). Over a dozen conformers with lowest energies were then subjected to final calculations using C-PCM solvent approximation. The local

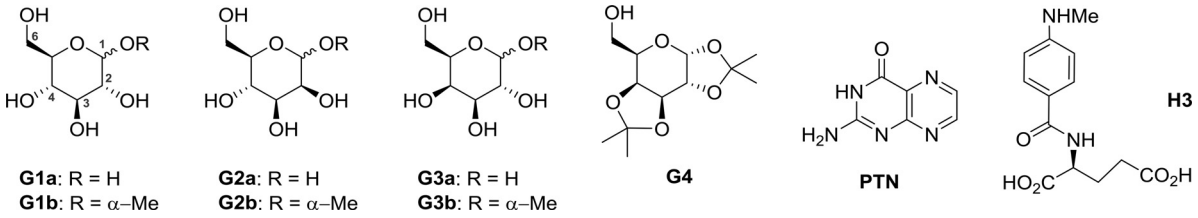

Fig. 2. Structures of studied D-hexoses (G1-G4) and model analogues of folic acid: 2-amino-4-hydroxy-pteridine (pterin, PTN) and N-[4-(methylamino)benzoyl]-L-glutamic acid (H3) evaluated in this study.

minima of the assemblies on the considered potential energy surface were verified by the harmonic frequency analysis.

2.5. Mass spectrometry measurements

The measurements and gas-phase stability data obtained from the collision experiments (CID analysis) were performed on 4000 QTRAP mass spectrometer (Sciex). The water/methanol mixture of **FA, PTN** or **H3** (c = 0.01–0.2 mM) and corresponding D-hexose (c = 0.1 mM) was infused to the electrospray ion source at a flow rate of 10 μL/min. The samples were analysed in both positive and negative ion modes with a capillary voltage at 4.2 V (-3.9 V), declustering potential of 20 V (-20 V), and entrance potential of 10 V (-10 V). The energy-resolved dissociation breakdown curves were recorded in multiple reaction monitoring (MRM) scanning modes. The nitrogen was used as a collision gas. In the MRM scanning mode the intensity of the peak corresponding to a given complex ion was monitored as a function of the increasing collision energy. The dissociation curves were prepared in SigmaPlot 12.0. The dissociation energy, defined as the center-of-mass collision energy (E_{cm}) at which the relative intensity of the complex ion is reduced to 50%, was obtained from sigmoidal relationship between E_{cm} and relative intensity of the complex ion. Each measurement was repeated three times. The reported dissociation energies are given in +/- 0.1 accuracy.

3. Results and discussion

3.1. Studies in solution (UV-Vis)

The studies in solution were performed using UV-Vis measurements and were carried out in biologically compatible buffer, namely phosphate buffered saline (PBS) at pH = 7.4. At this pH, the FA exists mainly as dicarboxylate anion [6] that shows two absorption maxima at 281 and 350 nm in the UV-Vis spectrum. We used UV-vis titration experiments for determining the stoichiometry of the obtained complexes as well as evaluating their association constants. Three simple hexoses: D-glucose (**G1a**), D-mannose (**G2a**) and D-galactose (**G3a**) were initially chosen as FA binding agents (Fig. 2).

In order to avoid dilution effects as well as the influence of a possible **FA** aggregation, **FA** concentration remained constant during experiments. In all cases, upon addition of carbohydrate aliquots the absorbance at the same wavelengths increased. Experimental data obtained from the UV-Vis titrations were fitted with HypSpec [28] program.

Different stoichiometries were tested (1:1, 1:2, 2:1 H:G), albeit simple 1:1 binding model gave the most accurate association constants (Table 1). Given that folic acid forms dimers in aqueous solutions [31] dimerization constant (K_d=6.6 ± 0.3 M^{-1}) [23b]. was included in calculations of association constants of folic acid/monosaccharides assemblies. All studied carbohydrates form associates with **FA** that have similar stabilities as expressed by comparable values of association constants (15 ± 0.1 for **FA**/**G1a**; 10 ± 0.1 for **FA**/**G2a**, and 10 ± 0.1 for **FA**/**G3a**).

Table 1
UV-Vis study of the host–guest interaction between PTN and carbohydrates[a].

Compound	K_a [M^{-1}]
D α glucose (G1a)	38 ± 0.8
methyl –α -D-glucoside (G1b)	40 ± 1.4
D α mannose (G2a)	31 ± 0.1
methyl -α -D-mannoside (G2b)	31 ± 0.1
D α α galactose (G3a)	39 ± 0.2
Methyl– α – D–galactoside (G3b)	32.4 ± 0.7
1,2:3,4-di-*O*-isopropylidene-α- D galactopyranose (G4)	<2

[a] Determined in phosphate buffered saline PBS, pH = 7.4) at 303 K.

The next part of our study was devoted to determination of which part of folate is responsible for the formation of supramolecular assembly with hexoses. In order to do that we divided **FA** into two model analogues: pterin (**PTN**) and N-[4-(*methylamino*)*benzo*yl]-L-glutamic acid (**H3**) (Fig. 2). For such obtained model subunits, the UV-Vis titration experiments under the same experimental conditions as for FA were performed (Table 1).

It was found that **H3** does not form supramolecular associates under studied conditions, whereas pterin (**PTN**) formed strong associates with **G1a, G2a, and-G3** hexoses. To evaluate the influence of anomeric hydroxyl group of hexose on the binding pattern with **PTN**, methyl α-D-glucoside (**G1b**), methyl α-D-mannoside (**G2b**), and methyl α-D-galactoside (**G3b**) were also evaluated (Fig. 2, Table 1).

The association constants do not differ either between associates of **PTN** with a specific carbohydrate and its substituted at anomeric position analogue – suggesting that hydroxyl group O(1)H is not essential for the binding of folate. To examine further this binding pattern a carbohydrate with only one free hydroxyl group O(6)H- 1,2:3,4-di-*O*-isopropylidene-α-D-galactopyranose (**G4**, Fig. 2) – was applied, resulting this time the significant reduction of the association costant (K_a < 2 M^{-1}). Such decrease in binding affinity confirms that either of O(2)H, O(3)H or O(4)H hydroxyl groups may be crucial for the binding. Additionally, the value of association constant obtained for the **G4-PTN** assembly confirms that O(6)H hydroxyl group of carbohydrate takes part in folate binding.

These results clearly indicate that pterin subunit is responsible for formation of associates, whereas the PABA-GLN moiety is not interacting at all with the carbohydrates.

3.2. Molecular modeling of supramolecular assemblies

To shed a light into molecular recognition mechanism leading to the formation of studied supramolecular assemblies we conducted additional theoretical calculations at DFT/B3LYP-D3/6-31G(d) level of theory. The influence of solvent was approximated using conductor-like polarizable continuum model (C-PCM). First we determined the relative stability of tautomers of pterin (**PTN**), and then the most-stable four tautomers of **PTN** (Fig. 3a) were subjected to conformational calculation analysis to determine the relative stabilities of **PTN-G3b** and **PTN-G4** supramolecular assemblies.

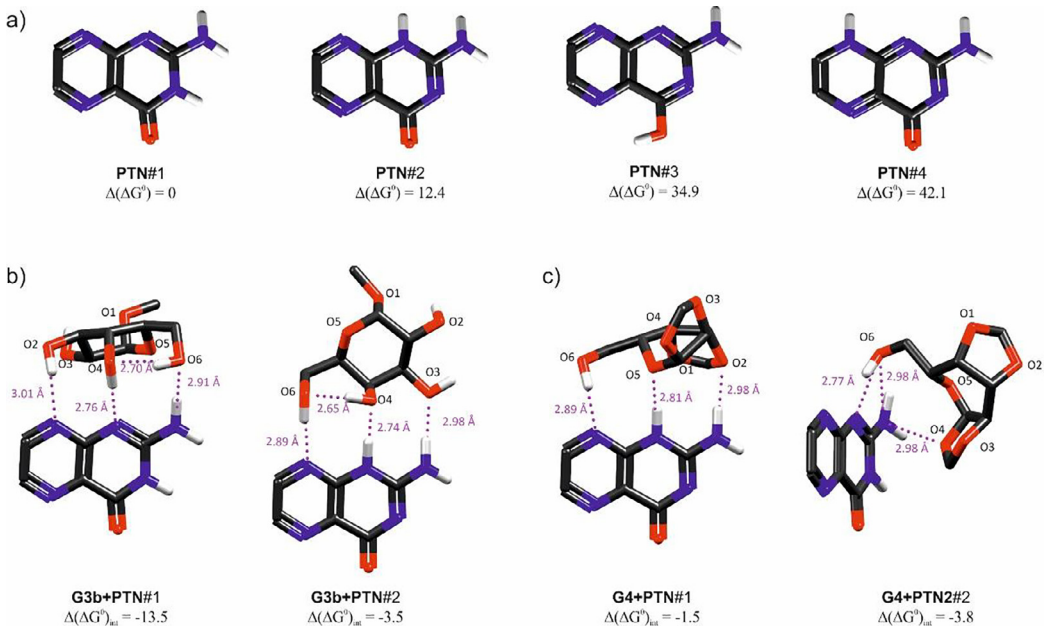

Fig. 3. Molecular structures and relative stabilities of pterin (PTN) and its supramolecular assemblies 199 with hexoses G3b and G4 calculated at DFT/B3LYP-D3/6-31G(d)/C-PCM:water level of theory: four 200 lowest-energy tautomers of PTN (a) and PTN associates with methyl α−D−galactoside (G3b) (b) and 1,2:3,4-di-O-isopropylidene-α-D-galactopyranose (G4) (c). The energies are given in kJ·mol-1 and ΔG0 201 at 298.15K; Δ(ΔG0)int = (ΔG0 complex − (ΔG0 hexose + ΔG0 202 pterin)); only assemblies of hexoses with tautomers of H2 having Δ(ΔG0 203)int > 0 are shown. Non-acidic protons were omitted for clarity.

The selected molecular structures and relative stabilities of these assemblies are depicted in Fig. 3b,c.

As it could be clearly seen from analysis of Fig. 3b in the **G3b**+**PTN** assemblies the partners are held together by three relatively short and directional hydrogen bonds involving two secondary (3-OH and 4-OH) and one primary (6-OH) hydroxyl groups acting as hydrogen bond acceptor and donor (d = 2.74−3.01 Å). In particular, only two pterin tautomers **PTN**#1 and **PTN**#2 were found to produce stable supramolecular associates with **G3b** ($\Delta(\Delta G^0)_{int}$ >0) with the **G3b**+**H2**#1 associate being the most stable one ($\Delta(\Delta G^0)_{int}$ = -13.5 kJ·mol^{-1}). In contrast, **PTN** and **G4** molecules interact only weakly due to formation of smaller number of less directional and longer hydrogen bonds (d = 2.77−2.98 Å). This is reflected by the low stabilities of the **G4**-**PTN** associates ($\Delta(\Delta G^0)_{int}$ up to 3.8 kJ·mol^{-1}). The results of DFT calculations correlate well with the UV-Vis measurements in aqueous buffer showing that **G4**-**H2** associates have low stabilities, at least in solution (vide infra), whereas **G1**-**G3** form relatively stable associates with **PTN** that have similar binding free energies (ΔG^0_{exp} ~ -8 kJ·mol^{-1}).

3.3. DSC and TG analyses of the supramolecular assemblies in the solid state

In order to examine if the investigated complexes could also be formed in the solid state, we performed additional Differential Scanning Calorimetry (DSC) and Thermogravimetric (TG) analyses [32] (in the range 25–300 °C, with heating rate 5° min^{-1}). As model compound and for comparison with previous investigations[23a] we chose folic acid and D-galactose. The DSC and TG curves for pure **FA** salt, galactose (**G3a**), and 1:1 and 1:5 (mol/mol) **FA**/**G3a** mixtures are shown in Fig. 4a and 4b, respectively.

The obtained TG and DSC plots of **FA**/**G3a** (1:5 mol/mol) mixture are clearly different from the obtained for parent compounds indicating the formation of the assembly which thermal properties differ significantly from the properties of pure **FA** and **G3a**. Specifically, the thermogram of **FA**/**G3a** (1:5) mixture showed two endothermic peaks (T_1 = 124 °C and T_2 = 143 °C). The latter peak corresponds to the melting of galactose (T_3 = 159 °C, the lit mp for galactose is 167 °C), which is the main component of the mixture, whereas the first peak is most likely related to the decomposition of the **FA**/**G3a** complex. This assumption is supported by the presence of preceding exothermic peak which indicates the solid to solid transition.

The weight loss in TG curves is caused by dehydration (under 150 °C) and decomposition of compounds (in the range 150–300 °C).

3.4. Identification and intrinsic stability studies of complexes of FA and its model analogues with hexoses by mass spectrometry approach

The selective formation of noncovalent associates between FA and its model subunits PTN and H3 with selected hexoses – galactose (**G3a**) and its derivatives: methyl α–*D*–galactoside (**G3b**) and 1,2:3,4-di-*O*-isopropylidene-α-D-galactopyranose (**G4**) was additionally studied using mass spectrometry (MS).

The MS analysis of the acidified water/methanol mixtures of **FA, PTN** and **H3** with selected hexoses revealed the presence of 1:1 associates in the case of both **FA** and **PTN**. Similarly to solution studies, compound **H3** was found to not form any associates with hexoses under studied conditions. The appropriate peaks corresponding to the protonated adduct ions were detected in the mass spectra recorded in the positive ion mode (Figs. S10 and S11). Additionally, some adducts were also observed as deprotonated species in the mass spectra recorded in the negative ion mode (Fig. S12). The higher-order aggregates were observed in MS experiments for FA solutions with D-galactose (**G3a**) and methyl α-D-galactoside (**G3b**). The summary of the ion species observed upon MS analysis is presented in Table 2.

The identity of the observed ionic associates was additionally confirmed by the analysis of their fragmentation pathways under collision-induced dissociation, CID (Fig. S4). CID of the protonated associates led to the protonated [**FA**+H]$^+$ or [**PTN**+H]$^+$ ions as the ionic fragment ions. Proton affinity (PA) of pterin (**PTN**), which is

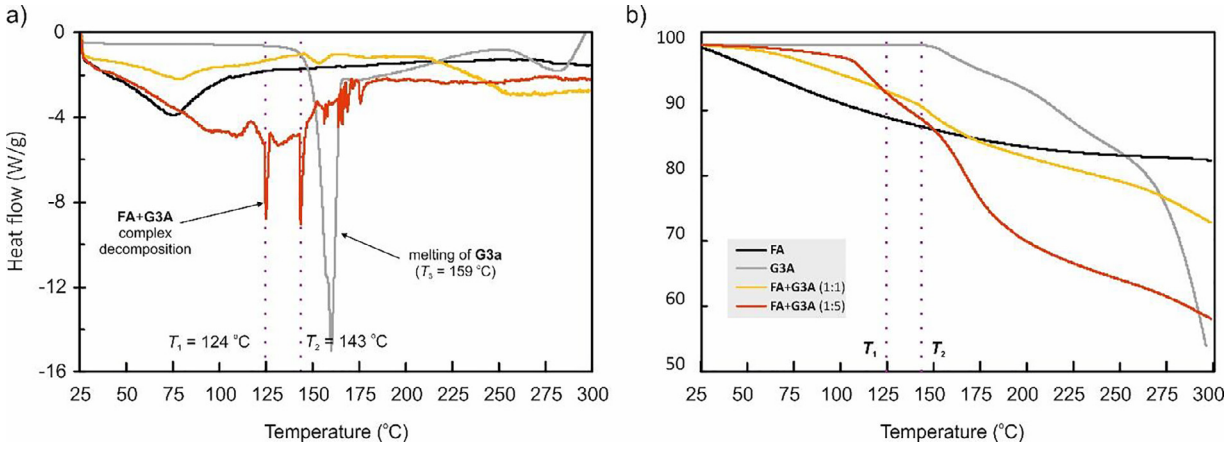

Fig. 4. Overlay of DSC (a) and TG (b) curves for FA (black line), D-galactose G3a (gray line), 1:1 (orange line) and 1:5 (red line) folic acid/galactose mixtures. (For interpretation of the references to color in this figure legend, the reader is referred to the web version of this article.)

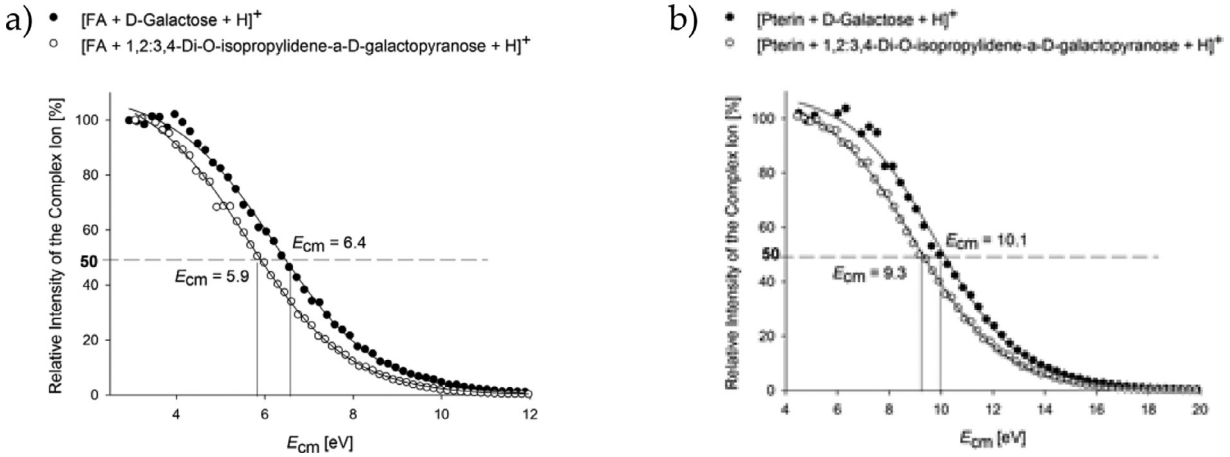

Fig. 5. Energy-resolved dissociation breakdown curves of protonated associates of folic acid (a) and pterin (b) with D-galactose (G3a) and 1,2:3,4-Di-*O*-isopropylidene-α-D-galactopyranose (G4). The E_{cm} represents the experimental dissociation energy of a protonated associate, i.e. the energy at which 50% of the complex dissociated.

Table 2
Mass spectroscopy identification of noncovalent assemblies of D-hexoses with FA and its subunit PTN[a].

D-Hexose	FA	PTN
G3a	$[G3a+FA+H]^+$	$[G3a+PTN+H]^+$
	$[2xG3a+FA+H]^+$	$[G3a+PTN-H]^-$
	$[G3a+FA-H]^-$	
	$[G3a+FA+Na-2H]^-$	
G3b	$[G3b+FA+H]^+$	$[G3b+PTN+H]^+$
	$[2xG3b+FA+H]^+$	$[G3b+PTN-H]^-$
	$[G3b+FA+Na-2H]^-$	
G4	$[G4+FA+H]^+$	$[G4+PTN+H]^+$

[a] Mass spectra were recorded in both positive and negative ion modes. The appropriate spectra are available in SI (Figs. S1–S3). No peaks corresponding to H3-hexoes assemblies were detected under studied conditions.

calculated to be 948.8 kJ mol^{-1} (see Fig. S16 for proton affinities of diferent pterin tautomers) is higher than the proton affinities of all three carbohydrates which were calculated to be: 870.1 kJ mol^{-1}, 877.6 kJ mol^{-1}, and 864.2 kJ mol^{-1} for **G3a, G3b**, and **G4**, respectively. Therefore, the protonated **FA** and pterin are the only ionic dissociation products observed in the CID spectra.

The intrinsic, gas-phase stabilities of the selected assemblies were determined by the analysis of their energy–resolved dissociation breakdown curves (Fig. 5), representing the relationship between applied, varied collision energy (E_{cm}) and intensity of the peak corresponding to protonated associate. The dissociation energy of the observed assembly was defined as the center of mass energy at which half of the associate underwent dissociation.

In the solvent-free environment both **FA** and pterin form the most stable complexes with D-galactose. The intrinsic stabilities given as the E_{cm} values are 6.6 and 10.1 eV, for **FA** and **PTN** associates, respectively. The complexes with **G4** – equipped with only one free hydroxyl group – are less stable than these with D-galactose (**G3a**). This results from distinct number of hydrogen bonds involved in the complex formation (Fig. 6).

Pterin (**PTN**) forms three strong hydrogen bonds with D-galactose (**G3a**), by being a donor of two hydrogen atoms and an acceptor of one hydrogen atom. In the case of the associate with **G4, PTN** is a donor of three hydrogen atoms, to make a three centered coordination operative. Though not shown here, the experimental dissociation energy of **PTN–G3b** complex was measured to be 9.7 eV. This value, which is slightly lower than that obtained for D-galactose (**G3a**) but significantly higher than for **G3b**, indicates that the primary hydroxyl group plays pivotal role in complex stabilization.

The bond lengths are substantially shorter for **PTN-G3a** associate. The calculated complexation energies of two associates (Fig. 4) well correlate with the experimental stability order. The complexes with FA reflect the general behavior observed for pterin

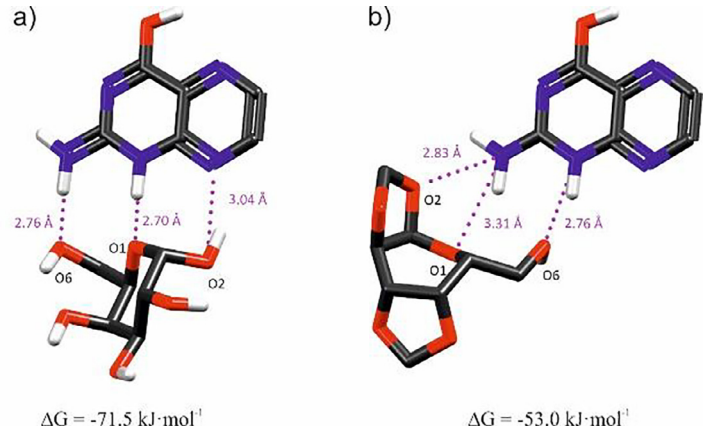

Fig. 6. The gas-phase structures of protonated assemblies [G3a+H_2+H]+ (a) and [G4+H_2+H]$^+$ (b) calculated at DFT/B3LYP-D3/6-311++(d,p) level of theory. Intermolecular hydrogen bonds and Gibbs free energies of complexation (at 298 K) are also shown, non-acidic protons were omitted for clarity.

complexes, although the stabilities are shifted to the lower values, similarly to that which is observed in solution.

4. Conclusions

Molecular recognition properties of folic acid by model D-hexoses (D-glucose, D-mannose, and D-galactose) was studied both in aqueous buffered solution (PBS, pH=7.4), in the gas phase, and in the solis state. Stabilities of the supramolecular assemblies were determined by the help of both experimental (UV-Vis, MS) and theoretical (DFT calculations) approaches. Moreover, structural motifs of D-hexoses and FA crucial for the assembly formation were identified. It was found that pterin subunit of FA is essential for the molecular assembly with hexoses, whereas PABA and GLN subunits of FA have virtually no effect on assembly formation. In solution, the most stable complexes were formed with hexoses having unprotected 3, 4, and 6 hydroxyl groups. The 1 and 2-hydroxyl groups were found to have less impact on the stability of the assemblies. Likewise, in the gas phase, the free hydroxyl groups of hexose were crucial for the formation of the associates with FA, albeit even one free hydroxyl OH6 was found to be enough to form the assembly.

The observation that simple hexoses bind folic acid by forming three directional hydrogen bonds between pterin part of FA and carbohydrate hydroxyl groups is a key step in the development of new molecular receptors for folic acid. Currently further studies aiming to strengthen the molecular interactions between FA and monosaccharide-based receptors are underway in our laboratory.

Declaration of Competing Interest

The authors declare that they have no known competing financial interests or personal relationships that could have appeared to influence the work reported in this paper.

Supplementary materials

Supplementary material associated with this article can be found, in the online version, at doi:10.1016/j.molstruc.2021.131904.

CRediT authorship contribution statement

Magdalena Ceborska: Conceptualization, Methodology, Validation, Formal analysis, Resources, Investigation, Data curation, Writing – original draft, Writing – review & editing. **Kajetan Dąbrowa:** Methodology, Software, Validation, Formal analysis, Investigation, Data curation, Writing – original draft, Writing – review & editing. **Jakub Cędrowski:** Investigation, Validation. **Magdalena Zimnicka:** Methodology, Validation, Formal analysis, Investigation, Data curation, Writing – original draft, Writing – review & editing.

References

[1] A.M. Gazzali, M. Lobry, L. Colombeau, S. Acherar, H. Azaïs, S. Mordon, P. Arnoux, F. Baros, R. Vanderesse, Stability of folic acid under several parameters. C, Eur. J. Pharm. Sci. 93 (2016) 419–430.
[2] (a) J. Sudimack, R.J. Lee, Targeted drug delivery via the folate receptor, Adv. Drug Deliv. Rev. 41 (2000) 147–162; (b) M. Ceborska, Folate appended cyclodextrinsfor drug, DNA, and siRNA delivery, Eur. J. Pharm. Biopharm. 120 (2017) 133–145; (c) A. Narmani, M. Rezvani, B. Farhood, P. Darkhor, J. Mohammadnejad, B. Amini, S. Refahi, N. Goushbolagh, Folic acid funcionalized nanoparticles as pharmaceutical carriers in drug delivery systems, Drug Dev. Res. 80 (2019) 404–424.
[3] N. Gonen, Y.G. Assaraf, Antifolates in cancer therapy: structure, activity and mechanisms of drug resistance, Drug Resist. Update 15 (2012) 183–210.
[4] J. Walling, From methotrexate to pemetrexed and beyond. A review of the pharmacodynamic and clinical properties of antifolates, Invest. New Drug 24 (2006) 37–77.
[5] W.T. Purcell, D.S. Ettinger, Novel antifolate drugs, Curr. Oncol. Rep. 5 (2003) 114–125.
[6] M.A. Hofsäss, J. Souza, N.M. Silva-Barcellos, K.R. Bellavinha, B. Abrahamsson, R. Cristofoletti, D.W. Groot, A. Parr, P. Langguth, J.E. Polli, V.P. Shah, T. Tajiri, M.U. Mehta, J.B. Dressman, Biowaiver monographs for immediate-release solid oral dosage forms: folic acid, J. Pharm. Sci. 106 (2017) 3421–3430.
[7] (a) D. Curiel, M. Más-Montoya, G. Sánchez, Complexation and sensing of dicarboxylate anions and carboxylic acids. Molecular recognition and sensing of dicarboxylates and dicarboxylic acids, Coord. Chem. Rev. 284 (2015) 19–66; (b) S.M. Butler, K. Jolliffe, Org. Biomol. Chem. 18 (2020) 8236–8254.
[8] (a) C. Miranda, F. Escartí, L. Lamarque, M.J.R. Yunta, P. Navarro, E. García-España, M.L. Jimeno, New 1H-pyrazole-containing polyamine receptors able to complex L-glutamate in water at physiological pH values, J. Am. Chem. Soc. 126 (2004) 823–833; (b) S. Carvalho, R. Delgado, M.G.B. Drew, V. Calisto, V. Félix, Binding studies of a protonated dioxatetraazamacrocycle with carboxylate substrates, Tetrahedron 64 (2008) 5392–5403.
[9] (a) C. Schmuck, M. Schwegmann, A naked-eye sensing ensemble for the selective detection of citrate—but not tartrate or malate—in water based on a tris-cationic receptor, Org. Biomol. Chem. 4 (2006) 836–838; (b) S.L. Wiskur, J.L. Lavigne, A. Metzger, S.L. Tobey, V. Lynch, E.V. Anslyn, Thermodynamic analysis of receptors based on guanidinium/boronic acid groups for the complexation of carboxylates, α-hydroxycarboxylates, and diols: driving force for binding and cooperativity, Chem. Eur. J. 10 (2004) 3792–3804.
[10] (a) S. Marullo, F. D'Anna, M. Cascino, R.J. Noto, Molecular "pincer" from diimidazolium salt: a study of binding affinity, J. Org. Chem. 78 (2013) 10203–10208; (b) A.L. Koner, J. Schatz, W.M. Nau, U. Pischel, Selective sensing of citrate by a supramolecular 1,8-naphthalimide/calix[4]arene assembly via complexation-Modulated pKa shifts in a ternary complex, J. Org. Chem. 72 (2007) 3889–3895.
[11] (a) M.H. Filby, S.J. Dickson, N. Zaccheroni, L. Prodi, S. Bonacchi, M. Montalti, M.J. Paterson, T.D. Humphries, C. Chiorboli, J.W. Steed, Induced fit interanion discrimination by binding-induced excimer formation, J. Am. Chem. Soc. 130 (2008) 4105–4113; (b) K. Ghosh, A.R. Sarkar, Anthracene-based macrocyclic fluorescent chemosensor for selective sensing of dicarboxylate, Tetrahedron Lett. 50 (2009) 85–88.

[12] (a) M.B. Jiménez, V. Alcazar, R. Pelaez, F. Sanz, A.L. Fuentes de Arriba, M.C. Caballero, Bis-amidocarbazolyl urea receptor for short-chain dicarboxylate anions, Org. Biomol. Chem. 10 (2012) 1181–1185; (b) D. Lichosyt, S. Wasiłek, J. Jurczak, Exploring the chiral recognition of carboxylates by C2-symmetric receptors bearing glucosamine pendant arms, J. Org. Chem. 81 (2016) 7342–7343.
[13] (a) S.Y. Liu, L. Fang, Y.B. He, W.H. Chan, K.T. Yeung, Y.K. Cheng, R.H Yang, Cholic-acid-based fluorescent sensor for dicarboxylates and acidic amino acids in aqueous solutions, Org. Lett. 7 (2005) 5825–5828; (b) S.Y. Liu, Y.B. He, W.H. Chan, A.W.M. Lee, Cholic acid-based high sensitivity fluorescent sensor for α,ω-dicarboxylate: an intramolecular excimer emission quenched by complexation, Tetrahedron 62 (2006) 11687–11696.
[14] (a) G.Y. Qing, Y.B. He, F. Wang, H.J. Qin, C.G. Hu, X. Yang, Enantioselective fluorescent sensors for chiral carboxylates based on calix[4]arenes bearing an L-tryptophan unit, Eur. J. Org. Chem. (2007) 1768–1778; (b) A. Mishra, V. Vajpayee, H. Kim, M.H. Lee, H. Jung, M. Wang, P.J. Stang, K.W. Chi, Self-assembled metalla-bowls for selective sensing of multi-carboxylate anions, Dalton Trans. 41 (2012) 1195–1201.
[15] (a) H. Maeda, Y. Fujii, Y. Mihashi, Diol-substituted boron complexes of dipyrrolyl diketones as anion receptors and covalently linked 'pivotal' dimers, Chem. Commun. (2008) 4285–4287; (b) R. Gotor, A.M. Costero, P. Gaviña, S. Gil, M. Parra, Binding and fluorescent sensing of dicarboxylates by a bis(calix[4]pyrrole)-substituted BODIPY dye, Eur. J. Org. Chem. (2013) 1515–1520.
[16] J.F. Davies, T.J. Delcamp, N.J. Prendergast, V.A. Ashford, J.H. Freisheim, J. Kraut, Pterin (H_2) forms three strong hydrogen bonds w Howell, E.W. Crystal structures of recombinant human dihydrofolate reductase complexed with folate and 5-deazafolate, BioChem 29 (1990) 9467–9479.
[17] E.W. Howell, Calorimetric studies of ligand binding in R67 dihydrofolate reductase, Biochem 44 (2005) 12420–12433.
[18] W. Welch, C.R. Sage, T.J. Stout, T. Klein, J. Ruppert, R.M. Stroud, A. Jain, Multi-targeted antifolates aimed at avoiding drug resistance form covalent closed inhibitory complexes with human and Escherichia coli thymidylate synthases, J. Mol. Biol. 313 (2001) 813–829.
[19] (a) K.M. Park, K. Suh, H. Jung, D.W. Lee, Y. Ahn, J. Kim, K. Baeka, K. Kim, Cucurbituril-based nanoparticles: a new efficient vehicle for targeted intracellular delivery of hydrophobic drugs, Chem. Commun. 73 (2009) 71–73; (b) Y.X. Chang, X.M. Zhang, X.C. Duan, F. Liu, L.M. Du, Supramolecular interaction of methotrexate with cucurbit[7]uril and analytical application, Spectrochim. Acta A 183 (2017) 131–137.
[20] K. Wang, Q.Q. Wang, M.N. Wang, S. Xing, B. Zhu, Z.H. Zhang, Supramolecular amphiphilic assembly formed by the complexation of calixpyridinium with alimta, Langmuir 35 (2019) 9020–9028.
[21] Y.V. Shalaeva, J.E. Morozova, V.V. Syakaev, A.M. Ermakova, I.R. Nizameev, M.K. Kadirov, E.K. Kazakova, A.I. Konovalov, Formation of cooperative amidoaminocalixresorcinarene - methotrexate nanosized aggregates in an aqueous solution and on the surface of gold nanoparticles, Supramol. Chem. 30 (2018) 901–910.
[22] D. Quiñonero, K.A. López, P.M. Deyà, M. Nieves Piña, J. Morey, Synthetic tripodal squaramido-based receptors for the complexation of antineoplastic folates in water, Eur. J. Org. Chem. (2011) 6187–6194.
[23] (a) M. Ceborska, M. Zimnicka, M. Pietrzak, A. Troć, M. Koźbiał, J. Lipkowski, Structural diversity in native cyclodextrins/folic acid complexes - from [2]-rotaxane to exclusion compound, Org. Biomol. Chem. 10 (2012) 5186–5188; (b) M. Ceborska, M. Zimnicka, M. Wszelaka-Rylik, A. Troć, Characterization of folic acid/native cyclodextrins host-guest complexes in solution, J. Mol. Struct. 1109 (2016) 114–118; (c) M. Zimnicka, A. Troć, M. Ceborska, M. Jakubczak, M. Koliński, W. Danikiewicz, Structural elucidation of specific noncovalent association of folic acid with native cyclodextrins using an ion mobility mass spectrometry and theoretical approach, Anal. Chem. 86 (2014) 4249–4255; (d) M. Ceborska, K. Kędra-Królik, A.A. Kowalska, M. Koźbiał, Comparative study of molecular recognition of folic acid subunits with cyclodextrins, Carbohydr. Polym. 184 (2018) 47–56.
[24] (a) D. Van Eker, S.K. Samanta, A.P. Davis, Biomimetic carbohydrate recognition, Chem. Soc. Rev. 49 (2020) 2531–2545; (b) C.M. Renney, G. Fukuhara, Y. Inoue, A.P. Davis, Binding or aggregation? Hazards of interpretation in studies of molecular recognition by porphyrins in water, Chem. Commun. 51 (2015) 9551–9554; (c) I. Banik, M. Roy, Structural effects of three carbohydrates in nicotinic acid/water mixed solvents, J. Mol. Liq. 203 (2015) 66–79; (d) M. Mazik, K. Cavga, Carboxylate-based receptors for the recognition of carbohydrates in organic and aqueous media, J. Org. Chem. 71 (2006) 2957–2963; (e) J. Lippe, W. Seichter, M. Mazik, Improved binding affinity and interesting selectivities of aminopyrimidine-bearing carbohydrate receptors in comparison with their aminopyridine analogues, Org. Biomol. Chem. 13 (2015) 11622–11632.
[25] E.J. Toone, Structure and energetics of protein-carbohydrate complexes, Curr. Opin. Struct. Biol. 4 (1994) 719–728.
[26] K. Kano, N. Tanaka, S. Negi, Hydrogen-bonded complexes of carboxylate anions and dextrins in an aprotic polar solvent, Eur. J. Org. Chem. (2001) 3689–3694.
[27] P. Moulik, A.K. Mitra, Association of carbohydrates with amines: part I. Proton donor-acceptor complexes of D-glucose, D-mannose, D-galactose, 2-amino-2-deoxy-D-glucose, and maltose with ethylenediamine, Carbohydr. Res. 23 (1972) 65–74.
[28] (a) P. Gans, A. Sabatini, A. Vacca, Investigation of equilibria in solution. Determination of equilibrium constants with the HYPERQUAD suite of programs, Talanta 43 (1996) 1739–1753; (b)Gans, P., Sabatini, A., Vacca, A. 2000, Hypspec, Leeds, UK, and Florence, Italy; (c) F. Ulatowski, K. Dąbrowa, T. Bałakier, J. Jurczak, Recognizing the limited applicability of job plots in studying host-guest interactions in supramolecular chemistry, J. Org. Chem. 81 (2016) 1746–1756; (d) D.B. Hibbert, P. Thordarson, The death of the Job plot, transparency, open science and online tools, uncertainty estimation methods and other developments in supramolecular chemistry data analysis, Chem. Commun. 52 (2016) 12792–12805.
[29] Spartan'18 Wavefunction, Inc. Irvine, CA, 2020.
[30] (a) A.D Becke, A new mixing of Hartree-Fock and local density-functional theories, J. Chem. Phys. 98 (1993) 1372–1377; (b) P.J. Stephens, F.J. Devlin, C.J. Chabalowski, M.J. Frisch, Ab initio calculation of vibrational absorption and circular dichroism spectra using density functional force fields, J. Phys. Chem. 98 (1994) 11623–11627.
[31] M. Abu Khaled, C Krumdieck, Association of folate molecules as determined by proton NMR: implications on enzyme binding, Biochem. Biophys. Res. Commun. 130 (1985) 1273–1280.
[32] M.E. Brown, P.K. Gallagher, Handbook of Thermal Analysis and Calorimetry: Applications to Inorganic and Miscellaneous Materials, Elsevier, 2003.